

## **Chapter 4: Micromachined Microbolometer Fabrication**

To realize the idea of a wavelength selective structure, surface and bulk micromachining techniques have been adopted. Several dielectric layers and a sacrificial layer are deposited and etched to construct the microbolometer structure. Fabrication method and related issues are discussed in this chapter.

### **4.1 Chromium as microbolometer material**

Comparing with Te, Bi, and popular material  $V_{ox}$ , chromium is much worse material due to 1-2 order smaller temperature coefficient of resistance (TCR) [1][2]. It also has oxidation problem. However, in 2-3 days after deposition oxidation of chromium is stabilized. The reason for adopting chromium is because it is easy and convenient to use. Chromium is deposited by e-beam evaporation at the rate of  $0.5 - 1 \text{ \AA/s}$ . At the thickness of  $300 \text{ \AA}$ , the sheet resistance, which is the ratio of resistivity by the film thickness, is around  $270 - 320 \text{ ohm/sqr}$ . This is about a 5 factor of higher than the bulk resistivity; typical resistivity values for Cr films deposited on glass substrates by thermal evaporation techniques are in the range of  $20-200 \text{ }\mu\Omega\text{-cm}$  [3]. The electrical resistivity and even negative and positive TCR of chromium are greatly influenced by various parameters such as substrate preparation, deposition technique, thickness of the film, temperature of substrate, and post deposition annealing [3][4].

## 4.2 The process for conventional micromachined microbolometer

Broadband microbolometer is fabricated for characterization of devices such as TCR, thermal impedance, and resistance over power dissipation. Figure 4.1 illustrates a schematic drawing of the fabrication procedure of a microbolometer on 4-inch single crystal (100) silicon wafers with 500  $\mu\text{m}$  thickness. Similar configuration of membrane supported by legs on silicon substrate is usually found in the conventional microbolometers for modern focal-plane-arrays (FPA) [5][6][7]. The only difference is the self-aligned structure for electrical isolation as shown in Fig. 4.1c. Even though the nature of a microbolometer is as a broadband detector, due to the dielectric layers beneath bolometer layer, there is a weak wavelength dependency as shown in Fig.3.6 of the previous chapter.

First, 750  $\text{\AA}$  of silicon nitride is deposited as a barrier layer for the silicon substrate in a reaction of ammonia ( $\text{NH}_3$ ) and dichlorosilane ( $\text{SiCl}_2\text{H}_2$ ) at a gas flow rate of 3.5:1 at 830  $^\circ\text{C}$ . This barrier layer is used to separate the silicon substrate and polysilicon, and it provides electrical isolation during the measurement.

After then, the LPCVD undoped polysilicon layer is deposited at 650  $^\circ\text{C}$  using silane ( $\text{SiH}_4$ ) and is patterned by 25  $\text{HNO}_3$ : 13  $\text{H}_2\text{O}$ : 1  $\text{HF}$  in volume having an etch rate of 1000  $\text{\AA}/\text{min}$ . Removing the sacrificial polysilicon between the top microbolometer structure and the bottom nitride film creates the air gap of 1  $\mu\text{m}$ . A sacrificial polysilicon layer provides the thermal isolation between microbolometer and substrate, which results in improving the thermal impedance.

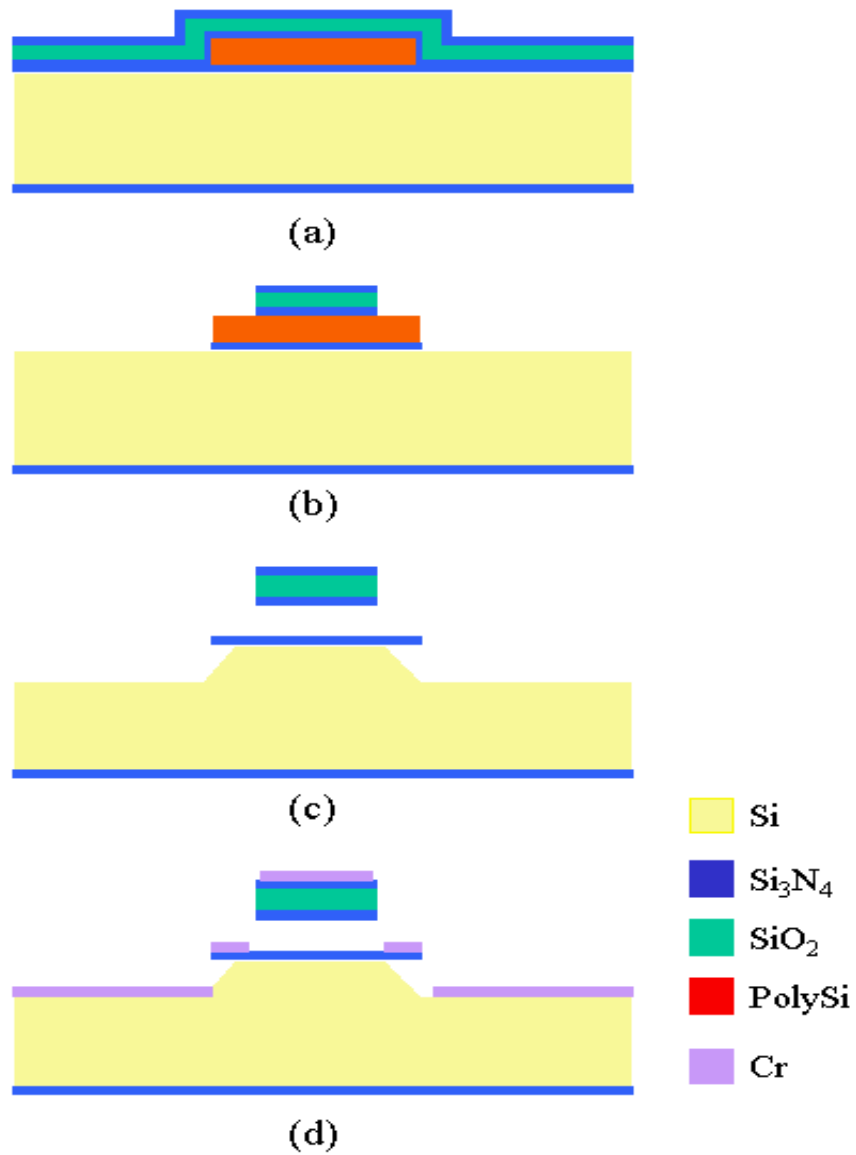


Figure 4.1 Schematic view of fabrication procedure: (a) deposition of silicon nitride, deposition and patterning of polysilicon, and deposition of top bolometer structure; (b) Etching bolometer structure and bottom silicon nitride; (c) Sacrificial poly silicon etching and forming self-aligned structure; (d) Deposition of Cr as bolometer layer.

Previous researchers reported that most of the thermal loss is generated through thermal conduction into substrate [5][6][7]. Once the polysilicon layer is removed, the air gap provides thermal isolation from the substrate.

The next step is to deposit the top dielectric layers over the patterned polysilicon. The top microbolometer structure consists of a multiple film stack of two silicon nitride layers cladding a silicon dioxide layer. The reason for the  $\text{Si}_3\text{N}_4\text{-SiO}_2\text{-Si}_3\text{N}_4$  multiple stack layers is to provide for the mechanical stability. The dielectric stack should not buckle or crack because of stresses (compressive stress and tensile stress). To minimize these stresses, a multiple film stack of two-silicon nitride layers cladding a silicon dioxide layer ( $\text{Si}_3\text{N}_4\text{-SiO}_2\text{-Si}_3\text{N}_4$  multiple stack layers) is used as a membrane. A 10000 Å silicon dioxide layer is sandwiched between two 1500 Å thick silicon nitride layers on the double-side polished wafer. Experimentally, the total thickness of membrane structure should be at least 5000 Å in order to survive during the sacrificial release process.

Silicon nitride is deposited in a reaction of ammonia ( $\text{NH}_3$ ) and dichlorosilane ( $\text{SiCl}_2\text{H}_2$ ) at a gas flow of 3.5:1 at 830 °C and 315mTorr. Silicon dioxide is deposited in a reaction of silane ( $\text{SiH}_4$ ) and oxygen ( $\text{O}_2$ ) at a gas flow rate of 1:10 at 460°C and 110 mTorr.

After depositing the top membrane, the microbolometer is directly patterned on the top membrane, and this allows access to the sacrificial polysilicon layers encapsulated by the top membrane and the bottom silicon nitride layer. Plasma etching is performed to pattern the microbolometer structure. Using  $\text{CF}_4$  and  $\text{O}_2$  with 100 watts power, reactive ionized etching (RIE) performs

the plasma etching of the silicon dioxide and silicon nitride layers. The etch rate of silicon dioxide and silicon nitride is observed to be about 700 Å /min and 1000 Å /min, respectively. Due to the thick top membrane and the oxygen containing recipe, the photoresist has to be thick enough to endure the long etch time. If AZ 5214 photoresist is coated at 4000 rpm for 40 second, the thickness of photoresist is around 1.4 μm. To establish a thicker photoresist, one more coating is applied, and the final photoresist has a thickness of 1.8 μm.

Except for the thin nitride layer covered by the sacrificial polysilicon layer, plasma etching is done until the bare silicon is revealed. The sacrificial polysilicon is partially revealed through the microbolometer pattern.

The sacrificial polysilicon is etched using KOH solution at 80 °C. Since the adjacent area of the device is etched down to bare silicon, KOH etches the silicon area as well. The undercutting process generates the overhanging structure as shown Figure 4.1c. The more detail result of a KOH etch simulated by Anisotropic Crystalline Etching Simulation (ACES) [8] is presented in Fig.4.2. Since the undercut separates the device from the plane wafer surface, the self-aligned structure for electrical isolation is realized after deposition of the bolometer material.

After forming the freestanding microbolometer structure supported by four legs, it is nearly impossible to perform other patterning processes. Therefore, the self-aligned structure gives the advantage of choosing any bolometer material that can be deposited or sputtered.

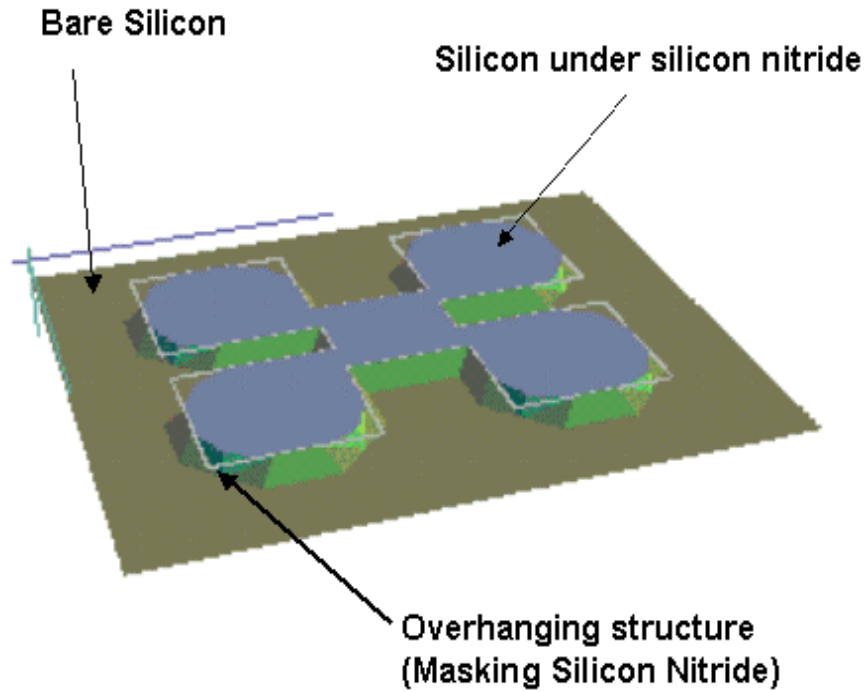


Figure 4.2 Self aligned structure simulated by Anisotropic Crystalline Etching Simulation (ACES) tool [8]. The bolometer structure is not shown in this figure.

After completion of the KOH etching process, the wafer is rinsed for 20 minutes in deionized (DI) water followed by 20 minutes in isopropyl alcohol before being dried. Finally, chromium is e-beam evaporated at the rate of 0.5 – 1 Å/s. An Inficon crystal monitor is used to measure the real time deposition rate and thickness. Because of the self-aligned structure, the device is ready right after chromium evaporation for electrical and optical measurement without requiring

any further metal patterning. Figure 4.3 shows the top view of the final microbolometer structures.

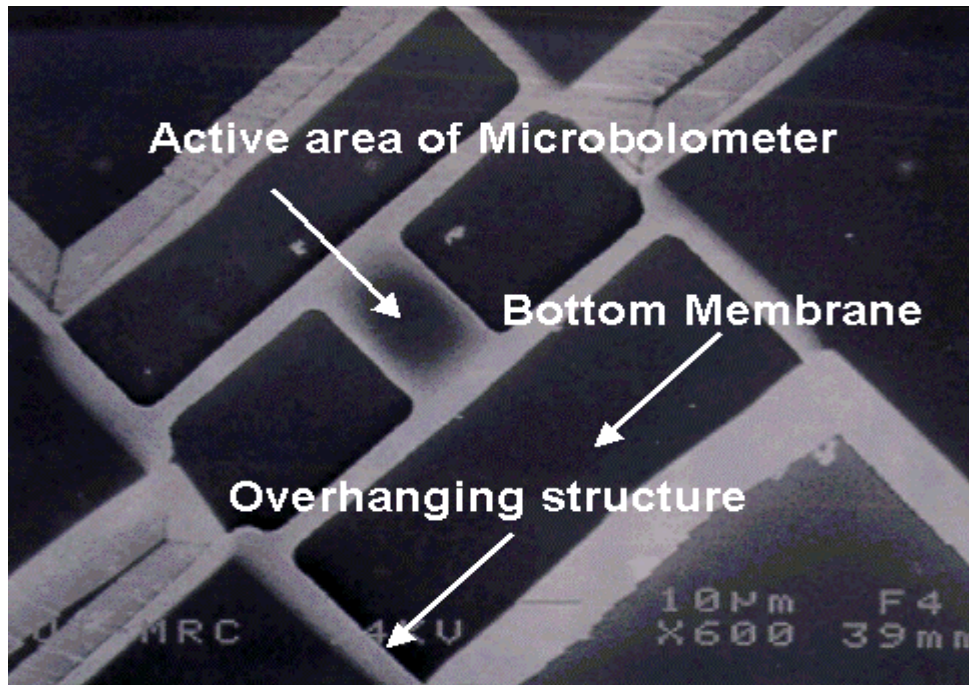


Figure 4.3 Top view of the fabricated conventional microbolometer.

#### **4.3 The Process for resonant dielectric cavity enhanced microbolometer**

Figure 4.4 shows a schematic drawing of the fabrication procedure of a resonant dielectric cavity enhanced microbolometer for wavelength selectivity. Comparing with the microbolometer structure in figure 4.1, the perfect mirror can be configured to enhance the absorption of incoming infrared with wavelength selectivity. Four-inch single crystal (100) double polished silicon wafers are used as substrates with thickness of 250  $\mu\text{m}$ . A 5020  $\text{\AA}$  of silicon dioxide layer is

sandwiched between 700 and 900 Å thick silicon nitride layers on the double side polished wafer. The layers are all deposited by LPCVD. All deposition is the same LPCVD recipe as mentioned in section 4.2. The thickness of each film can be determined according to the targeted wavelength. Comparing with conventional microbolometer and resonant air cavity microbolometer, the structure of resonant dielectric cavity microbolometer has more robust mechanical configuration due to not having sacrificial layer to form the freestanding structure. Therefore, selection of thickness of dielectric film is less sensitive in terms of mechanical stability.

After depositing multiple film layers on a wafer, the dielectric film stack on the backside of the double polished wafer is patterned and plasma etched. Before the plasma etching, the wafer must be coated with photoresist on the front side of the wafer to avoid unintentional etching during plasma etching. After etching the pattern, the remaining backside multi-layer stack becomes a masking layer for the subsequent wet KOH silicon anisotropic etching. The silicon substrate is anisotropically etched using 40% KOH solution at 110°C. The averaged etch rate of the (100) silicon is about 1 μm/min at 110°C. This etch rate is very sensitive to the solution temperature; therefore, a stable temperature should be maintained during etching to insure repeatable etch times.

After forming the membrane on the structure, the microbolometer structure is patterned and plasma etched. However, before the plasma etching, the backside of the films has to be coated with photoresist. Without the protective coating layer, a small amount of overetching can easily cause the device to fail.



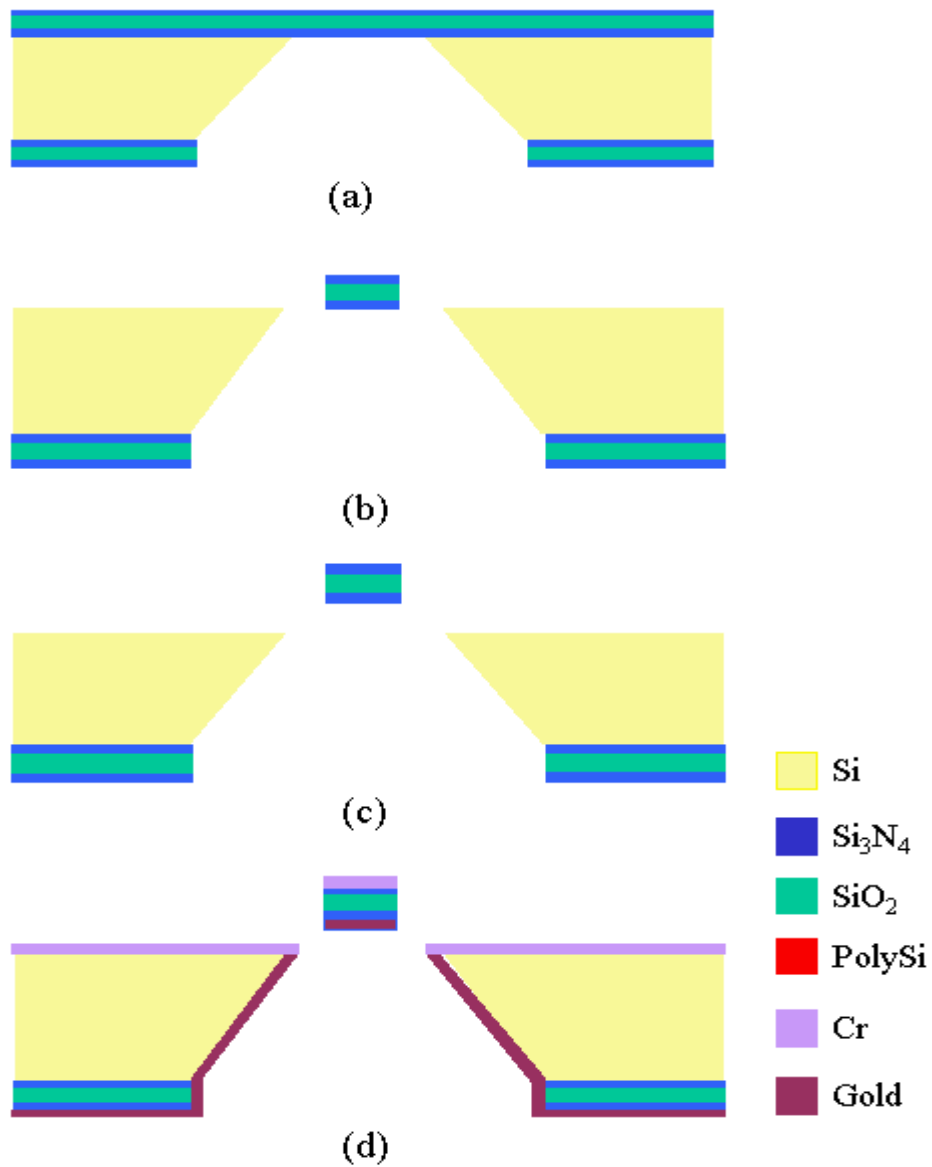


Figure 4.4 Schematic view of fabrication procedure: (a) formation of membrane; (b) Patterning the microbolometer using RIE; (c) forming self-aligned structure (d) Deposition of chromium on the top surface and deposition of gold as mirror layer.

To make the self-aligned structure for electrical isolation in measurement, the sample is immersed into KOH solution at 80 °C. This KOH etching process generates the overhanging structure as shown in figure 4.2. Before depositing the bolometer material and mirror layer on the back, the sample must be cleaned thoroughly. After completion of KOH etching process, the wafer is rinsed 20 minutes in deionized (DI) water and then 20 minutes in isopropyl alcohol before being dried. Figure 4.5 demonstrates the resonant dielectric cavity microbolometer.

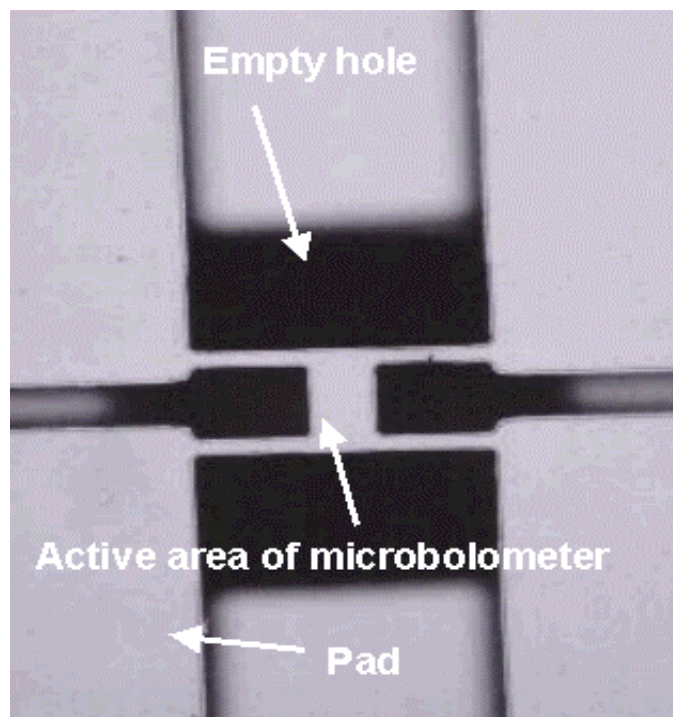


Figure 4.5 The top view of fabricated resonant dielectric cavity enhanced microbolometer (50 x 10 optical picture).

Finally, chromium is e-beam evaporated at the rate of  $0.5 - 1 \text{ \AA/s}$ . After optical measurement with this configuration, gold is deposited at  $0.5 - 1 \text{ \AA/s}$  as mirror layer. Deposition of bolometer and mirror layer forms the Fabry Perot structure using a dielectric cavity.

Due to single bottom membrane, the shortest wavelength of first resonance is around 6 micron. This should be suitable to detect from the mid wave infrared (MWIR) ( $3 - 5 \text{ }\mu\text{m}$  wavelengths) and longer wave infrared.

#### **4.4 The process for resonant air cavity enhanced microbolometer**

Figure 4.6 contains diagrams that show the procedure for the fabrication of a resonant air cavity enhanced microbolometer. Unlike the previous devices, the cavity of this device consists of air and dielectrics. The base of the device is the usual 4 inch single crystal (100) double polished silicon wafer with thickness of  $250 \text{ }\mu\text{m}$ . The membrane consists of two silicon nitride layers with thickness of  $750 \text{ \AA}$  and a  $5020 \text{ \AA}$  of silicon dioxide layer embedded in between the nitride layers. All of the mentioned films are deposited by LPCVD. The wavelength selectivity of each device can be adjusted by varying the thickness of each film, and of course, the ratio of each film's thickness has to be decided in order to provide the mechanical stability. The entire deposition recipe is identical to the deposition method described in section 4.2.

After depositing the multiple film layers on a wafer, the dielectric film stack on the backside of wafer is plasma etched. It is very important to note that the other side of the wafer must be protected from unintentional etching during

plasma etching; hence, it is covered with photoresist. After the desired pattern is achieved, the remaining backside multi-layer stack becomes a masking layer for the subsequent wet KOH silicon anisotropic etching.

The silicon substrate is anisotropically etched using 40% KOH solution at 110 °C to form the bottom membrane. After the KOH etching, the sacrificial polysilicon layer is deposited using LPCVD and etched using RIE. One crucial factor of the sacrificial layer patterning is that the area of the polysilicon squares has to be larger than that of the membrane; otherwise, the bottom membrane will fail to survive the undercutting process. If the polysilicon squares are smaller than the membrane, the bottom membrane itself will fall down during the self-aligned process.

Afterwards, the top membrane is deposited with the same recipe described in section 4.3. A 5000 Å thick silicon oxide layer is deposited between two 750 Å thick silicon nitride layers on the double side polished wafer by LPCVD. After the construction of the top membrane, all the layer stacks on the back side of the wafer, including the sacrificial dielectric silicon dioxide and nitride layers, are removed by multiple blanket wet etching and plasma etching steps. As before, the layout of the microbolometer is directly patterned on the top membrane, and the polysilicon is etched using KOH etchant. At the end, both the top and bottom membranes are released to form the Fabry Perot structure.

Once the self-aligned structure is finished, chromium is evaporated by e-beam evaporator at the rate 0.5 ~ 1 Å /s. Then gold is deposited at 0.5 ~ 1 Å /s as the mirror layer. As this point fabrication of the device is completed.

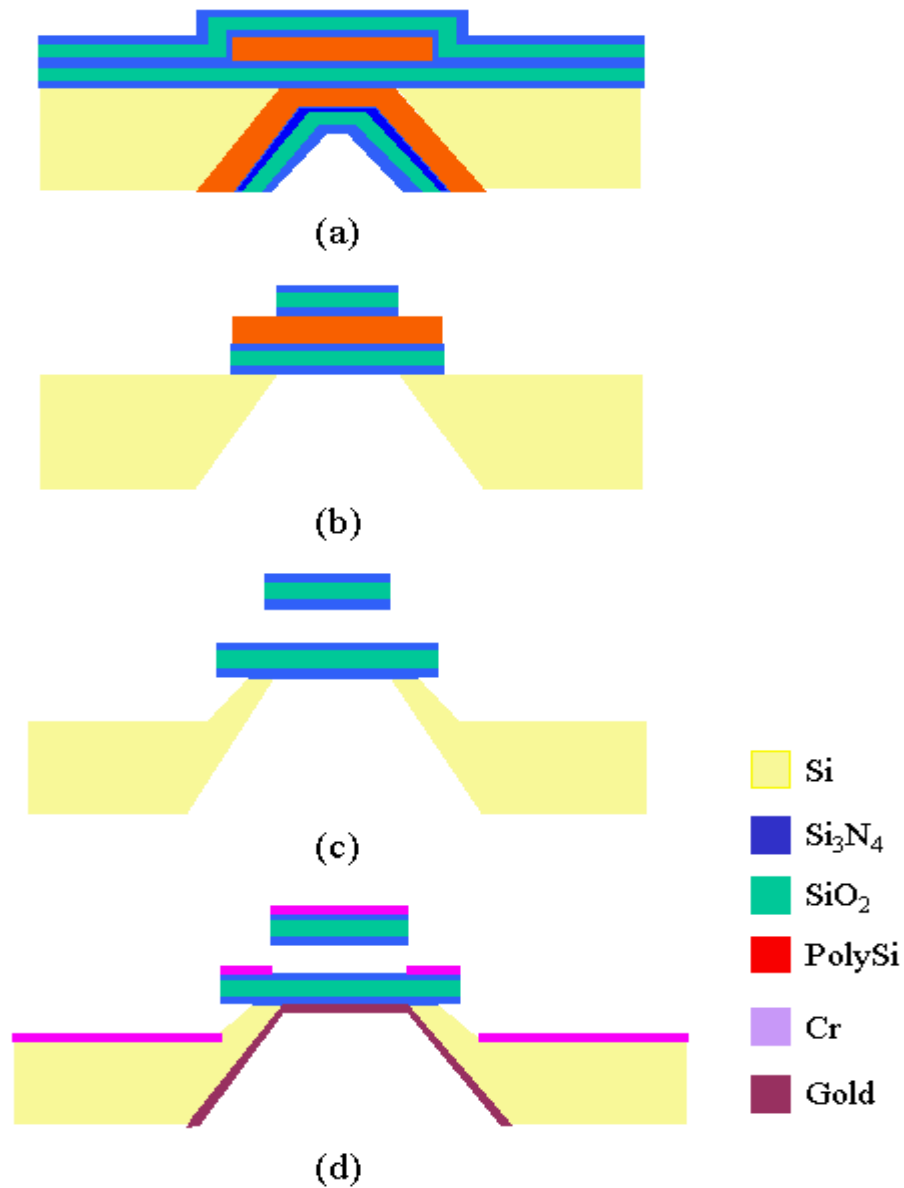


Figure 4.6 Schematic view of fabrication procedure: (a) formation of top and bottom membrane with forming sacrificial polysilicon layer; (b) Patterning the top membrane for microbolometer using RIE; (c) releasing the top and bottom membrane and forming the self-aligned structure (d) Deposition of chromium on the top surface and deposition of gold as mirror layer.

It should be noted that all the thickness as of each layer are determined for wavelength selectivity and mechanical stability of the membrane. Since both the top and bottom membrane are used, the minimum value of first resonance coupling is around 10  $\mu\text{m}$  due to physical limitation imposed by mechanical stability.

#### 4.5 Fabrication Issues

To achieve the suspended microbolometer structure, it is important to have mechanically stable dielectric properties. Figure 4.7 contains a picture of a broken leg, which is supposed to support the membrane. It is broken due to mechanical stress (3  $\mu\text{m}$  of width and 20  $\mu\text{m}$  of length). Young's modulus and residual stress in the films are two key mechanical properties of a membrane. The actual mechanical properties of the films are strongly influenced by deposition methods and conditions [9]. For a given radius of curvature stress of the film is obtained from the following equations [10][11],

$$\mathbf{s} = \frac{E}{1-\mathbf{n}} \cdot \frac{l_{sub}^2}{l_{film}} \cdot \frac{1}{6R} \quad (4.1)$$

where  $l_{film}$  is the thickness of the film,  $l_{sub}$  is the thickness of the substrate,  $R$  is the radius of curvature (negative for compressive stress and positive for tensile stress), and  $\nu$  is Poison's ratio of the substrate.

A membrane made of a multiple film stack has an advantage over a single film membrane in term of stress minimization even though it increases the complexity of the process. Stress minimization can be achieved by combining the tensile nature of the silicon nitride and the compressive nature of the silicon dioxide. Total residual stress of the stack should be weak tensile stress to allow the membrane to remain flat after completion of the devices in case of conventional microbolometer and resonant air cavity microbolometer. Han experimentally determined that the ratio of the silicon dioxide thickness to the silicon nitride thickness is optimized at about 3 to 3.5 [12]. With the ratio of 3 to 3.5, the residual stress of the composite membrane is 0.1 to 0.3 GPA. At the ratio of 2, excessive tensile stress may cause multi stack films to crack. At the ratio of 5, excessive compressive stress may cause buckling [12]. Equivalent residual stress of multiple stack films is determined from the following equation [13].

$$\sigma_{eq} = \frac{\sum_i (\sigma_i \cdot h_i)}{\sum_i h_i}$$

where  $\sigma_i$  is residual stress of the  $i_{th}$  film.

Because the stress is concentrated at the edge of the suspended leg, analytical calculation of stress for structure is very difficult. Therefore, various leg designs have been evaluated in this study. Experimentally, the membrane

structure with thickness of less than 5000 Å cannot withstand the sacrificial releasing process due to handling issue.

Another very challenging issue for making MEMS microstructures is stiction. Stiction is a general term describing the adhesion of the microstructure to the adjacent structures. During the rinse and dry cycle after the sacrificial etching process the evaporating rinse solution creates forces that draw the microstructure toward the underlying substrate. If the device structure comes in contact with the substrate, substantial attractive forces can develop between the two surfaces. For large size or low spring constant devices, this attractive force can easily exceed the restoring force of structure. As a consequence, the microstructure will remain adhered to the wafer surface after the rinse and dry cycle is completed.

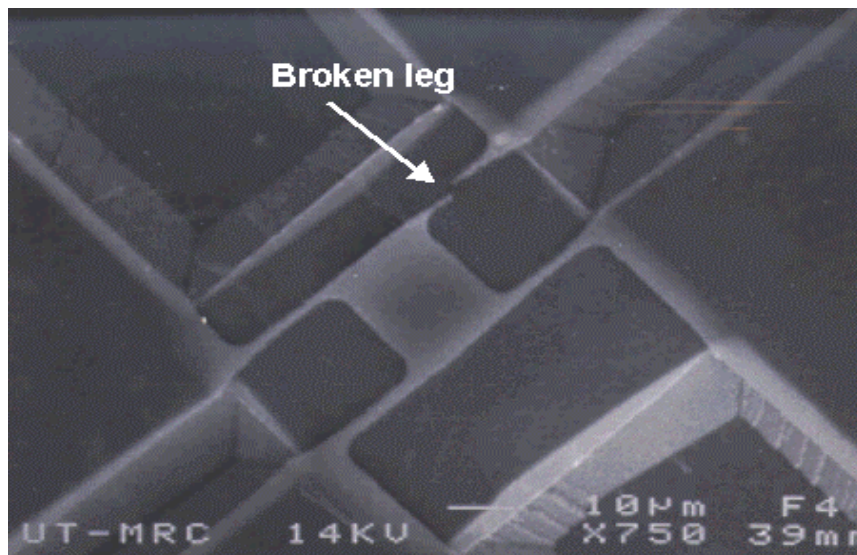


Figure 4.7 The crack of overetched legs caused by the residual tensile stress (3 µm width and 20 µm length legs).



Capillary forces dominate at tens of micron dimensions and processes have been developed to reduce or eliminate the forces for successful fabrication of MEMS structures [14]. Figure 4.8 illustrates this capillary force related to the surface characteristics. Hydrophobicity raises the H<sub>2</sub>O contact angle above 90 degrees creating a repulsive force between adjacent layers. One of the easiest ways to reduce the capillary force is to apply a solution with low surface tension during air-drying. For releasing of large and complex MEMS structure, several methods have been developed. For example, hydrophobic self-assembling monolayer coatings (SAMS Coating) can be deposited to achieve hydrophobic surface [15].

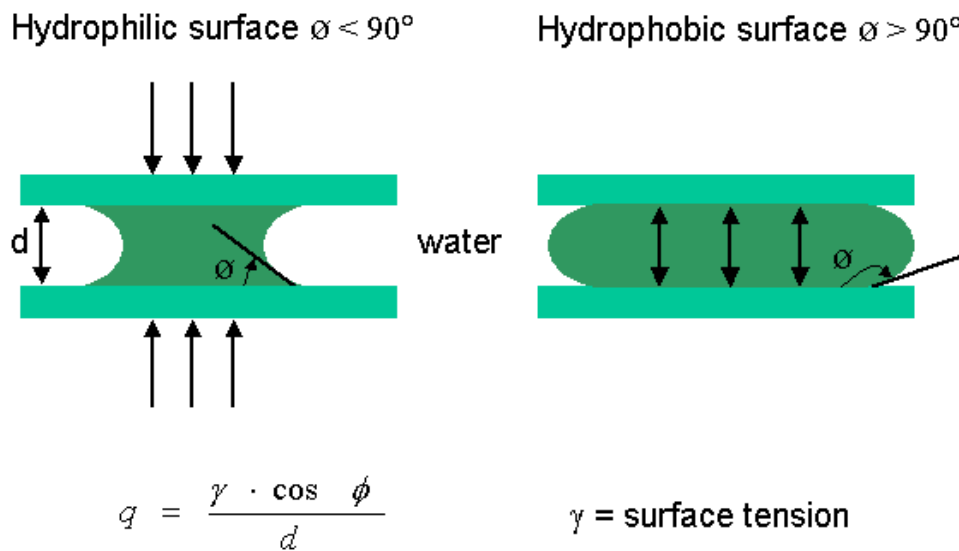


Figure 4.8 Capillary forces related the surface status [15].

An alternate approach to prevent the formation of a meniscus is by eliminating the liquid phase in figure 4.9 in the drying process. The two methods of achieving this are supercritical CO<sub>2</sub> drying (SCCO<sub>2</sub>) [8] and freeze sublimation [9]. In supercritical CO<sub>2</sub> drying method, after the water between two layers is exchanged to methanol, liquid CO<sub>2</sub> kept above the critical pressure (1073 psi) is used to dissolve and remove methanol under pressure. Once methanol is completely removed, the temperature in the vessel is raised above the critical temperature of CO<sub>2</sub> (31.1C), and the vessel is vented. Since a liquid-vapor interface was not found, capillary force is unable to bring adjacent surfaces into contact with one another, and stiction cannot be formed.

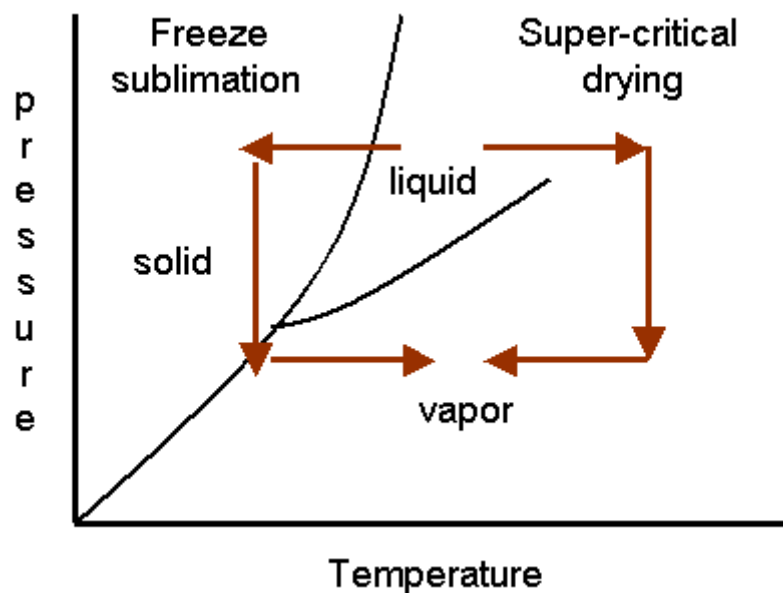


Figure 4.9 Phase diagram illustrating two paths to pass from the liquid to vapor state without encountering a liquid vapor interface [14].

In this research, there is a sacrificial layer etching and releasing process to form the broadband and resonant air cavity enhanced microbolometer. To reduce the capillary force, isopropyl alcohol (IPA) is used instead of water before the air-drying process, which improves the yield dramatically. With water drying, most of the devices failed during the releasing process.

#### **4.6 Summary**

The fabrication method of three different microbolometers was explained in this chapter. A broadband microbolometer was fabricated for characterization of devices for such characteristics as TCR, thermal impedance, and resistance versus power dissipation. A resonant dielectric cavity enhanced microbolometer with wavelength selectivity was built on a single membrane for wavelength selectivity. Due to the single bottom membrane, it is possible to achieve a minimum of first resonance around 6 microns. It should be suitable to detect the mid wave infrared (MWIR). The first resonance of resonant air cavity enhanced microbolometer is intrinsically higher due to the top and bottom membrane. All three fabrications processes produce a self-aligned structure for electrical isolation, which is not necessary for further patterning of bolometer layer.

Finally, mechanical stability and stiction, which are some of the most challenging problems in MEMS, fabrication were discussed, and a method of preventing those difficulties was introduced.